J. Biochem. 2011;149(3):293–300 doi:10.1093/jb/mvq143

JB THE JOURNAL OF BIOCHEMISTRY

Crucial effect of the first CXXC motif of human QSOX 1b on the activity to different substrates

Received October 26, 2010; accepted November 18, 2010; published online December 9, 2010

Wenyun Zheng[1,2,*], Yanyan Chu[2,*], Qin Yin[1,2], Lei Xu[1,2], Charles Yang[1,2], Wenyao Zhang[1,2], Yun Tang[2,†] and Yi Yang[1,2,‡]

[1]State Key Laboratory of Bioreactor Engineering, [2]School of Pharmacy, East China University of Science and Technology, 130 Meilong Road, Shanghai 200237, China

*These authors contributed equally to this work.

[†]Yun Tang, School of Pharmacy, East China University of Science and Technology, 130 Meilong Road, Shanghai 200237, China. Tel/Fax: +21 6425 1052, email: ytang234@ecust.edu.cn

[‡]Yi Yang, School of Pharmacy, East China University of Science and Technology, 130 Meilong Road, Shanghai 200237, China. Tel: +21 6425 1311, Fax: +21 6425 1287, email: yiyang@ecust.edu.cn

Among all sulphhydryl oxidases involved in disulphide formation, quiescin-sulphhydryl oxidase (QSOX) is unique for its multidomain structure, protein thiol oxidation activity and highly efficient catalysis. In this study, site-directed mutagenesis and molecular modelling methods were integrated to investigate the structural and functional characteristics of QSOX, especially the importance of the three CXXC motifs. Site-directed mutagenesis suggested that the C449–C452 motif was essential for the activity of human QSOX 1b; the C70–C73 motif was fundamental in electron transfer from thiol-containing substrate including reduced proteins, DTT, GSH rather than the phosphine-based thiol reductant TCEP, to the C449–C452 motif; and the C509–C512 motif was not involved in electron transfer during disulphide formation. The different roles of the CXXC motifs indicated that there were discrepant electron transfer pathways for the oxidation of thiol-containing substrates and non-thiol disulphide reductants. Molecular modelling method was then used to draw a reasonable picture for the electron transfer process and to elucidate the mechanism of electron transfer when different substrates were oxidized, which will greatly enhance our understanding of the action mechanism of QSOX.

Keywords: electron transfer/molecular modelling/QSOX/site-directed mutagenesis/thiol oxidation.

Abbreviations: ALR, augmenter of liver regeneration; DTT, dithiothreitol; Ero1, endoplasmic reticulum oxidoreductin 1; Erv1, essential for respiration and viability 1; GSH, glutathione; HsQSOX1b, human quiescin sulphhydryl oxidase 1 isoform b; IPTG, isopropyl-β-D-thiogalactopyranoside; β-ME, β-mercaptoethanol; PDI, protein disulphide isomerase; rRNase A, reduced ribonuclease A; TCEP, tris[2-carboxyethyl] phosphine; Trx, thioredoxin.

The flavoprotein quiescin-sulphhydryl oxidase (QSOX) is the only multidomain sulphhydryl oxidase that can insert disulphide bonds into unfolded or reduced proteins directly. QSOX exists in metazoan and some other single-cell organisms, but not in yeast. Although rat seminal vesicle sulphhydryl oxidase, a member of the QSOX family, was the first flavin-dependent sulphhydryl oxidase described (*1*), most of the mechanistic studies on these enzymes were based on the avian egg white QSOX (*2–6*).

QSOX consists of four domains, two thioredoxin-like domains, namely Trx1 and Trx2, a region called Spacer, which was predicted to be helix-rich regions (HRR), and an Erv/ALR FAD-binding domain (*7–9*). Human QSOX 1 isoform b (HsQSOX1b) contains three typical CXXC motifs: C70–C73 motif in the first thioredoxin-like domain (Trx1), C449–C452 motif in the Erv/ALR domain, and C509–C512 motif downstream of the Erv/ALR domain. In 2003, Thorpe and co-workers demonstrated that HsQSOX1b required all the three CXXC motifs to fulfil its catalysis (*3*). And then they suggested that C509–C512 motif was dispensable for oxidizing rRNase or dithiothreitol, while C70–C73 and C449–C452 motifs had important effects on the activity of QSOX (*10*). However, the exact functions of the three CXXC motifs and the Spacer domain are still unclear.

Elucidation of the functions of these CXXC motifs in QSOX is essential in order to understand the mechanism of disulphide formation and protein folding in eukaryote. Therefore, studies on the structure and function of QSOX are very important and challenging. On one hand, QSOX is probably the most complex and efficient thiol oxidase; on the other hand, different domains in QSOX may have different functions in the formation of disulphide bonds. Until now, the crystal structure of the full-length QSOX is not available yet, which seriously hinders the understanding of its biological function.

In this study, the function of conserved thiol groups in recombinant HsQSOX1b was analysed by site-directed mutagenesis and enzymatic assays with

different substrates. Part of the 3D structure of HsQSOX1b was then modelled and the interaction of HsQSOX1b with its substrates was investigated for the first time. The results suggest that the three CXXC motifs in HsQSOX1b play distinct roles and that different electron transfer pathways exist in the process of the oxidation of thiol-containing substrates and non-thiol disulphide reductant tris[2-carboxyethyl] phosphine (TCEP) as a special substrate of thiol oxidase.

Methods

Cloning of HsQSOX1b and mutants

HsQSOX1b cDNA clone (GenBank accession no. 4447666) from human kidney mRNA was obtained from Openbiosystems (www.openbiosystems.com, USA) in pCMV–SPORT6 vector. The desired cDNA was amplified by PCR with an N-terminal forward primer omitting the signal sequence 5′-tatcatatg gccccgcggtcggcgctctattcgcctt-3′ (NdeI site underlined) and a C-terminal reverse primer incorporating a stop codon 5′-caggcggccgc*tca*aataagctcaggtccctcag-3′ (stop codon italicized, NotI site underlined). The construct was directly ligated into pGEM-T TA cloning vector and identified correctly, then digested with restriction enzymes. The insert including an N-terminal hexahistidine tag was then ligated into the expression vector pET28a digested with NdeI and NotI.

The HsQSOX1b mutants were obtained by site-directed mutagenesis (QuikChange, Stratagene). All the primers used in this study in site-directed mutations are as follows: C70A–C73A mutation forward primer 5′-ggagttcttcgcctcctgggccggccacgccatcgccttcgccc-3′, C70A–C73A mutation reverse primer 5′-gggcgaa ggcgatggcgtggccggcccaggaggcgaagaactcc-3′; C449A–C452A mutation forward primer 5′-gcactacttcttcg gcgcccgagacgccgctagccacttcg-3′, C449A–C452A mutation reverse primer 5′-cgaagtggctagcggcgtctcgggcgccga agaagtagtgc-3′; C509A–C512A mutation forward primer 5′-ggccaccccgtgaacttgcttctgccgcccacaatgaacgc-3′, C509A–C512A mutation reverse primer 5′-gcgttcatt gtgggcggcagaagcaagttcacggggtggcc-3′. All constructs were fully sequenced to verify mutations and ensure that no additional changes had been introduced in the sequence.

Expression and purification of HsQSOX1b and mutants

Expression of HsQSOX1b and its mutants in *Escherichia coli* were first performed in BL21 DE3 cells at 37°C. Cells were grown to 0.6 of A_{600} and induced with 1 mM IPTG for 12 h, which resulted in the production of insoluble target proteins. To obtain a high yield of soluble active proteins enough to prove the character of the target enzyme, the construct was transformed into the Rosetta DE3 strain (Novagen). Cultures were grown in LB media supplemented with chloramphenicol and kanamycin. Over-expression of HsQSOX1b protein was induced at 18°C for 24 h with 0.3 mM IPTG and 10 μM FAD. The cells were harvested and resuspended with buffer A (50 mM sodium phosphate, 10 mM imidazole, 500 mM NaCl, pH 7.0) for purification.

The cells harvested in buffer A were disrupted by sonication and clarified by centrifugation at 10,000 rpm for 20 min at 4°C. Using an AKTA Purifier (GE) the supernatant was loaded to Histrap columns (GE) previously equilibrated in buffer A. The absorbed enzyme was eluted with a 0–100% gradient mixture from buffer A to buffer B (50 mM sodium phosphate, 500 mM NaCl, 500 mM imidazole, pH 7.0) in 10 column volumes. The eluted protein fractions were collected and incubated with FAD for 24 h. The pooled protein fractions were loaded onto Hitrap SP columns and eluted with 0–1 M NaCl gradient. Active fractions were pooled and ultrafiltrated against 100 mM sodium phosphate, with 300 mM NaCl, pH 7.0. The purity of target proteins was >90% as determined by 10% SDS–PAGE analysis.

Activity determination of HsQSOX1b and its mutants and comparison with other thiol oxidases

Activity assays were performed at 25°C in 50 mM potassium phosphate buffer at pH 7.5 containing 0.3 mM EDTA in a BioTek synergy 2 multifunction microplate reader (USA) according to a continuous fluorescence assay method (*11*) used thiol-containing small molecules DTT, GSH, β-ME, cysteine, homocysteine and reduced protein rRNase and non-thiol disulphide reductant TCEP as substrates. Recombinant HsQSOX1b (18 nM) and other thiol oxidases such as Ero1, Erv1 and Erv2 were determined with the final assay mixture containing 1 mM HVA, 1.4 μM horseradish peroxidase and 5 mM thiol from DTT, GSH, β-ME, cysteine, homocysteine or 5.7 mM TCEP or 300 μM rRNase. Kinetic data was obtained by monitoring the fluorescence product, produced with 360 nm excitation and 485 nm emissions, every 30 sec for 10 min. Control experiments were run in the absence of enzymes. The molar concentration of above recombinant enzymes were decided according to the molecular weight determined with size exclusion chromatography and molar extinction coefficient from ExPASy proteomics server (http://www.expasy.org/). Computation formula was as Eq. 1, where ε represents the molar extinction coefficient.

$$\text{Molar concentration} = A_{280}/\varepsilon \qquad (1)$$

Molecular modelling of HsQSOX1b

The primary sequence of HsQSOX1b was obtained from UniprotKB (*12*) (Accession No. O00391). According to the predicted results obtained from the DomPred Protein Domain Prediction Server (*13*), sequence number 30–156 (Trx1 domain), was modelled using the Modeller 9v4 (*14*). The crystal structure of yeast PDI [PDB code: 2B5E (*15*)] was retrieved from the Protein Data Bank. The a' domain of PDI (sequence number: 365–482) was selected and used as the template. The sequence alignment between the template and the target was carried out by ClustalW 1.83 (*16*) using a gap penalty of 10 and PAM series weight matrix. Five models were generated by Modeller 9v4

and validated by Procheck (*17*). The best structural model was chosen for further minimization and refinement. Two disulphide bonds between C70 and C73, C101 and C110 were assigned manually. Given the electron transfer between Trx1 and Erv/ALR, the modelled Trx1 structure and the recently known crystal structure containing Spacer and Erv/ALR domains of human QSOX1b protein [PDB code: 3LLI (*18*)] were docked by HADDOCK (*19*, *20*). The best docking solution was then submitted to PATCHDOCK (*21*, *22*), docking with monomer RNase (PDB code: 1W4O).

Meanwhile, the HADDOCK results were processed by adding hydrogen atoms and minimized to RMSD 0.3 Å using OPLS_2005 force field by Protein Preparation Wizard. The energy minimization of the model was then performed in three steps by MacroModel (*23*): firstly minimizing hydrogen atoms by constraining heavy atoms, then minimizing side chain with backbone constrained and finally relaxing the whole system. Both steepest descent and Polak–Ribiere conjugate gradient methods were applied for energy minimization in each step. Each stage was minimized by 500 steps of the steepest decent minimization followed by 4,500 steps of conjugate gradient minimization.

The minimized structure was then used to predict the location of the primary substrate binding site by SiteMap (*24*). TCEP and DTT were docked into the predicted pocket centred on residues C70 or C449 using the program Glide (*25*).

Results and Discussion

Activity comparison of different thiol oxidases

Besides N-terminal His-tagged HsQSOX1b, other typical thiol oxidases including Ero1-Lα, Erv1 and Erv2 were expressed in Rossetta DE3 cells and purified. Among all thiol oxidases studied, QSOX showed the highest disulphide forming activity, which was 100-, 200- and 300-fold higher than Erv2, Erv1 and Ero1-Lα when assayed with TCEP as disulphide reducing agent and 200-, 40- and 40-fold higher when assayed with DTT as disulphide reducing agent (Table I). It oxidized the protein substrate rRNase equally and efficiently as compared with small-molecule disulphide reducing substrates, while other thiol oxidases, Erv2, Erv1 and Ero1-Lα, could barely catalyse the oxidation of protein thiols. However, the recombinant HsQSOX1b almost could not oxidize other thiol-containing small molecular reductants except DTT and GSH (Table II). These data, consistent with previous report of chicken egg QSOX (*4*), suggest that QSOX is a unique protein thiol oxidase that is highly specialized in oxidizing the reduced protein. We therefore analysed QSOX activity by studying three types of substrates, thiol-containing small molecular reductants DTT, GSH and thiol-containing macromolecular reductant rRNase and non-thiol disulphide reductant TCEP. Compared with other thiol oxidases mentioned above QSOX had higher catalytic efficiency, the reason for which may be that QSOX is a multi-domain structure and the additional Trx domain probably is important for interacting with thiol-containing disulphide reductants DTT, GSH and rRNase, but not essential to non-thiol disulphide reductant TCEP. So the single-domain proteins Ero1-Lα, Erv1 and Erv2, containing no Trx domain, possess very low activities for substrate oxidation.

Up-to-date, several methods, such as oxygen consumption assay and thiol titration, was used to determine thiol oxidation activity. An improved, easy and accurate continuous fluorescence assay, using DTT as disulphide reducing agent, was recently reported by Raje *et al.* (*11*). The assay by Raje *et al.* (*11*) was based on enzymatic coupling of thiol oxidation to HRP mediated oxidation of HVA by H_2O_2, products of thiol oxidation. However, the assay was complicated by the fact that DTT, or other small molecular thiol-containing compounds, could react with H_2O_2 decreasing the sensitivity of reaction. Herein, we used the phosphine-based reductant TCEP instead of DTT as the disulphide reducing agent to detect the activity of QSOX. Moreover, we obtained higher response and a very good linear reaction curve (Fig. 1A). Because TCEP, a non-thiol reducer used as the disulphide reducing agent, readily reduced disulphide by the valency change of its core phosphorus from 5^+ to 3^+ and doesn't react with H_2O_2, avoiding the consumption

Table II. Activity Comparison of QSOX on different substrates.

Substrate (5 mM thiol)	TN min^{-1} of QSOX
TCEP	1,455 ± 53
DDT	576 ± 19
GSH	180 ± 8
β-ME	0
Cysteine	0
homo Cysteine	3 ± 0.5

TN, turnover numbers are reported as thiols oxidized.

Table I. Activity Comparison of HsQSOX1b, Ero1-Lα, Erv1 and Erv2.

Protein	5.7 mM TCEP TN min^{-1}	Relative T	5 mM DTT TN min^{-1}	Relative TN	300 μM rRNase TN min^{-1}	Relative TN
HsQSOX1b	1,455 ± 53	1.0000	576 ± 19	1.00	1,144 ± 249	1.0000
Ero1-Lα	4 ± 0.6	0.0029	15 ± 2	0.026	0.3 ± 1	0.0002
Erv1	6 ± 0.2	0.0041	15 ± 3	0.026	0	0
Erv2	12 ± 0.3	0.0084	3 ± 0.3	0.005	0.4 ± 0	0.0003

TN, turnover numbers are reported as thiols oxidized.

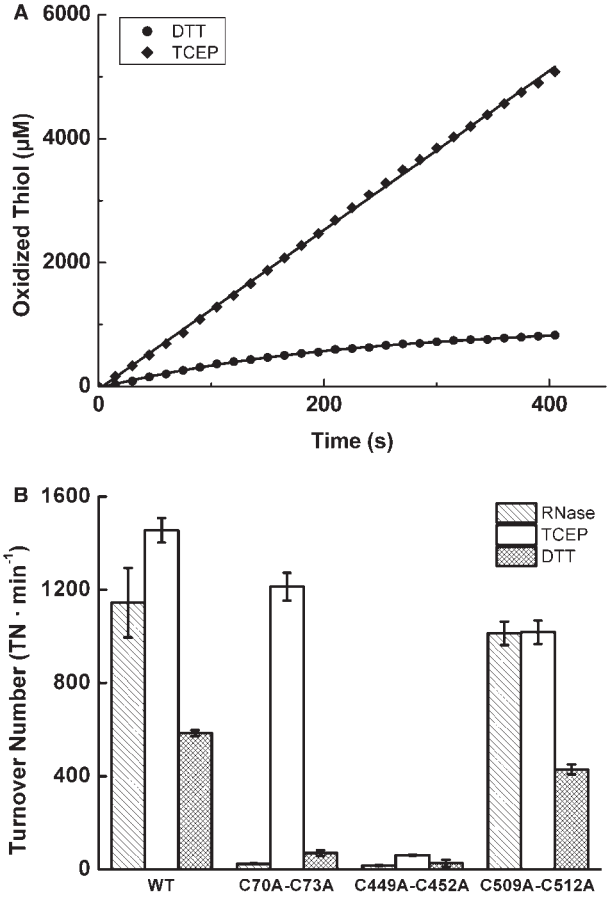

Fig. 1 The sensitivity of continuous fluorescence assay (A) and activity comparison of HsQSOX1b and its mutants on thiol-containing substrates DTT and rRNase and non-thiol substrate TCEP (B). (A) TCEP and DTT were used as substrates for continuous fluorescence assay, respectively. TCEP was oxidized by QSOX and the other thiol oxidase, and the linearity and accuracy of continuous fluorescence assay using TCEP as its substrate was better than DTT. (B) Activity comparison for wild-type and mutants of HsQSOX1b using DTT, rRNase and TCEP as substrate. The recombinant HsQSOX1b has the high activity to DTT, rRNase and TCEP. The mutant C70A–C73A kept the high activity to TCEP but very low activity to DTT and rRNase, 70, 1.4 and 1% of the wild-type activity. The C449A–C452A mutant almost lost the whole activity to DTT, rRNase and TCEP. The mutant C509A–C512A had comparatively minor effects on the activity to DTT, rRNase or TCEP, retaining 77, 89 and 83% of the wild-type activity.

of H_2O_2 produced by substrate oxidized, ensuring the higher response and the good linearity of reaction curve. Therefore, we suggested TCEP could be used as substrate to determine the activity of thiol oxidase, even a better substrate in increasing the sensitivity.

Activity of HsQSOX1b mutants

Three conserved CXXC motifs of HsQSOX1b were mutated separately to examine their roles in thiol oxidation. The C509–C512 motif seemed to be not functionally important, because a mutation of C509–C512 showed little effect on oxidative activity, keeping 77, 89 and 83% of the wild-type activity to DTT, rRNase and TCEP. Mutation of the C70–C73 motif located in the Trx1 domain of HsQSOX1b retained most of its activity toward non-thiol disulphide reducer TCEP, while this mutant lost its activity towards thiol-containing substrate rRNase and DTT, remaining 70, 1 and 1.4% of the wild-type activity, respectively (Fig. 1B). These results were primarily consistent with the previous study on HsQSOX1b, in which the mutations C70 or C73 in Trx1 domain resulted in the loss of most of its *de novo* disulphide formation activity towards small molecular substrates like DTT and protein substrates (*10*). However, in the results it was surprised that the way by which QSOX oxidized TCEP was completely different from the other substrates adopted, which was less affected by the Trx1 domain. Mutants of the conserved CXXC motifs within the Erv/ALR domain of HsQSOX1b (C449–C452) lost its activities on not only DTT, rRNase but also TCEP (Fig. 1B), which was consistent with previous studies on Erv1 (*26*), Erv2 (*27*) and Q6 (*4*, *9–11*, *26*, *27*). This also indicated that C449–C452 motif played essential roles in directing electron transfer to non-covalent bound FAD and then to oxygen. To confirm the above findings, homology modelling and protein–protein docking methods were integrated and the interactions of HsQSOX1b with its substrates were analysed.

Construction and refinement of HsQSOX1b model

HsQSOX1b, whose full-length protein structure was not available until now, is a multidomain sulphhydryl oxidase. The functional essential modules were the Trx1 domain and the Erv/ALR domain. After searching the database, structure homologies with Trx2 domain was not retrieved. And Spacer and Erv/ALR domains were crystallized recently (*18*). Therefore, only the Trx1 domain was modelled. The sequence similarity was 41.4% between Trx1 domain and the template a' domain of yeast PDI. Sequence alignment was shown in Fig. 2A. Secondary structures were marked under the sequences.

The stereochemical quality of the model was validated by Procheck. The best model was shown in the Ramachandran plot. There were 93.3% residues located in the core region and 6.7% in the allowed region (Fig. 2B). The validation results indicated that the quality of the models was quite reasonable and reliable. To investigate the function and interaction of the three CXXC motifs, Trx1 domain was docked to 3LLI (*18*).

Structural features of HsQSOX1b

QSOX is composed of two thioredoxin domains (Trx1 and Trx2), a Spacer and an Erv/ALR flavin-binding domain, which contains an essential redox-active CXXC motif adjacent to FAD (*7*, *28*). Trx1 domain adopted the thioredoxin fold with minor variations (Fig. 3A). The secondary structure elements were arranged in the order $\beta_1\alpha_1\beta_2\alpha_2\beta_3\alpha_3\alpha_4\beta_4\alpha_5$, and the catalytically active CGHC motif was located at the N-terminus of the second α-helix. Till now, there were no structures which were sequence homologous with Trx2. Erv/ALR domain, homologous with Erv2p, together with Spacer was recently crystallized (*18*). It is highly helical with C449–C452 located in the vicinity

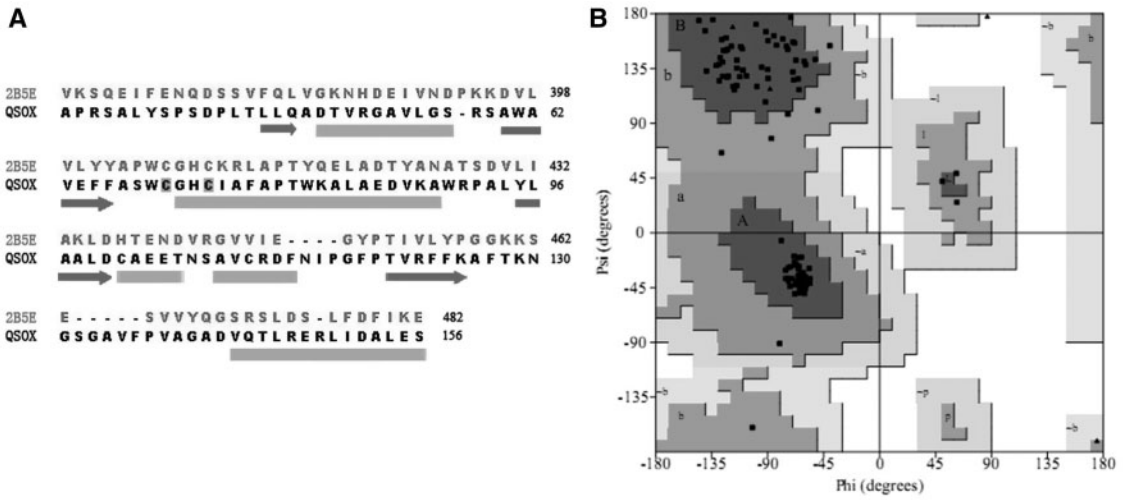

Fig. 2 Sequence alignment and evaluation of models. (A) Sequence alignment between sequences of templates. Secondary structures were marked under the sequences. The number in both-side columns is the corresponding residue number. Cysteines forming CXXC motifs were marked with dark background. (B) The Ramachandran Plot of Trx1 module. There were no residues located in disallowed region.

of the isoalloxazine ring of FAD, opposite to the active CXXC motif of Trx1 (Fig. 3A). The residues in Erv/ALR involved in aromatic ring stacking with FAD were His481 and Trp408, almost the same as those in Erv2p (*7*) (Fig. 3B). The aromatic ring stacking was believed to be responsible for the fold. The fusion of thioredoxin with FAD-linked Erv/ALR domains (*29–31*) demonstrated a significant advantage on catalytic efficiency in the oxidation of protein substrates compared to other thiol oxidases that only share Erv/ALR domain in the oxidation of protein substrates. Meanwhile, the fusion allowed HsQSOX1b to transfer electron easily via flavin and finally to oxygen, which lead to the production of stoichiometric H_2O_2 (*3*, *32*).

In the Trx1 and the known structure of QSOX1 docking results (Fig. 3A, C), disulphides which were formed by C70–C73 and C449–C452 were located face to face, resulting in C70–C73 and C449–C452 orientated inside. The minimum distance of S in both motifs was ~7Å. The active site prediction showed that there was a probable binding site located around the C449–C452 motif (Fig. 3E), while the pocket around the C70–C73 motif was hydrophobic, small and shallow (Fig. 3D). The docking processes were performed centred on residues C70 and C449, and choosing Trx1 and 3LLI as the starting structures, respectively.

The results showed that the pocket around C70 of Trx1 domain was too small and hydrophobic to bind TCEP (Fig. 3D). Moreover, the conformation of TCEP was quite extended, and the reactive atom of TCEP was in the centre of the extended conformation, which made it hard that TCEP binded to Trx1. As to DTT, it is smaller than TCEP, and not as extended as TCEP. DTT can bind to Trx1 majored by H-bonded to H72 and F403 (Fig. 3D). The pocket of Erv/ALR domain was adjacent to the FAD cofactor, and it was much bigger and deeper than the one around C70–C73 (Fig. 3E). TCEP could bind to Erv/ALR tightly with its terminal carboxylate forming H-bond with C449, R401 and F403 and electrostatic interaction with R318 and R450. The distance of the reactive P atom of TCEP and S of C449 is about 5–6 Å. The distance facilitates the electron transfer from TCEP to disulphide. The docking results showed that C449–C452 motif was essential for oxidizing TCEP substrate, though the interaction mechanisms had some difference.

Protein–protein docking of RNase and QSOX did not define the binding site of the two enzymes specially. PATCHDOCK docked RNase to the whole surface of QSOX automatically. The docking results showed that RNase tend to bind with Trx1 domain. The most frequent binding modes of RNase docking showed that the Trx1 domain played an important role in binding protein substrates (Fig. 3C). C70–C73 was located closer to the cysteine residue of the RNase than the C449–C452 motif. This is in agreement with the fact that mutation of C70A–C73A resulted in loss of QSOX's activity on proteins. Thanks to the particular position, C449–C452 plays a decisive role in its activities. Because C509–C512 was distal from the active centre, it did not have great effects on QSOX's activities on both small molecule and protein substrates.

The experimental results and the molecular modelling gave concordant results. C509–C512 was not necessary for QSOX's activities. C449–C452 was related to activities including disulphide formation activity and protein thiol oxidase activity. C70–C73 is essential for HsQSOX1b's disulphide formation activity toward the studied thiol-containing substrates, and greatly affected the activity of its protein thiol oxidase. This was concordant with the previous study on HsQSOX1b in which the mutations C70 or C73 in Trx1 domain resulted in the loss of most of its *de novo* disulphide formation activity toward small molecular substrates like DTT (*10*).

Different electron transfer pathway of QSOX

Given the computation and mutation results and the proposed mechanism by Thorpe's group (*33*), we

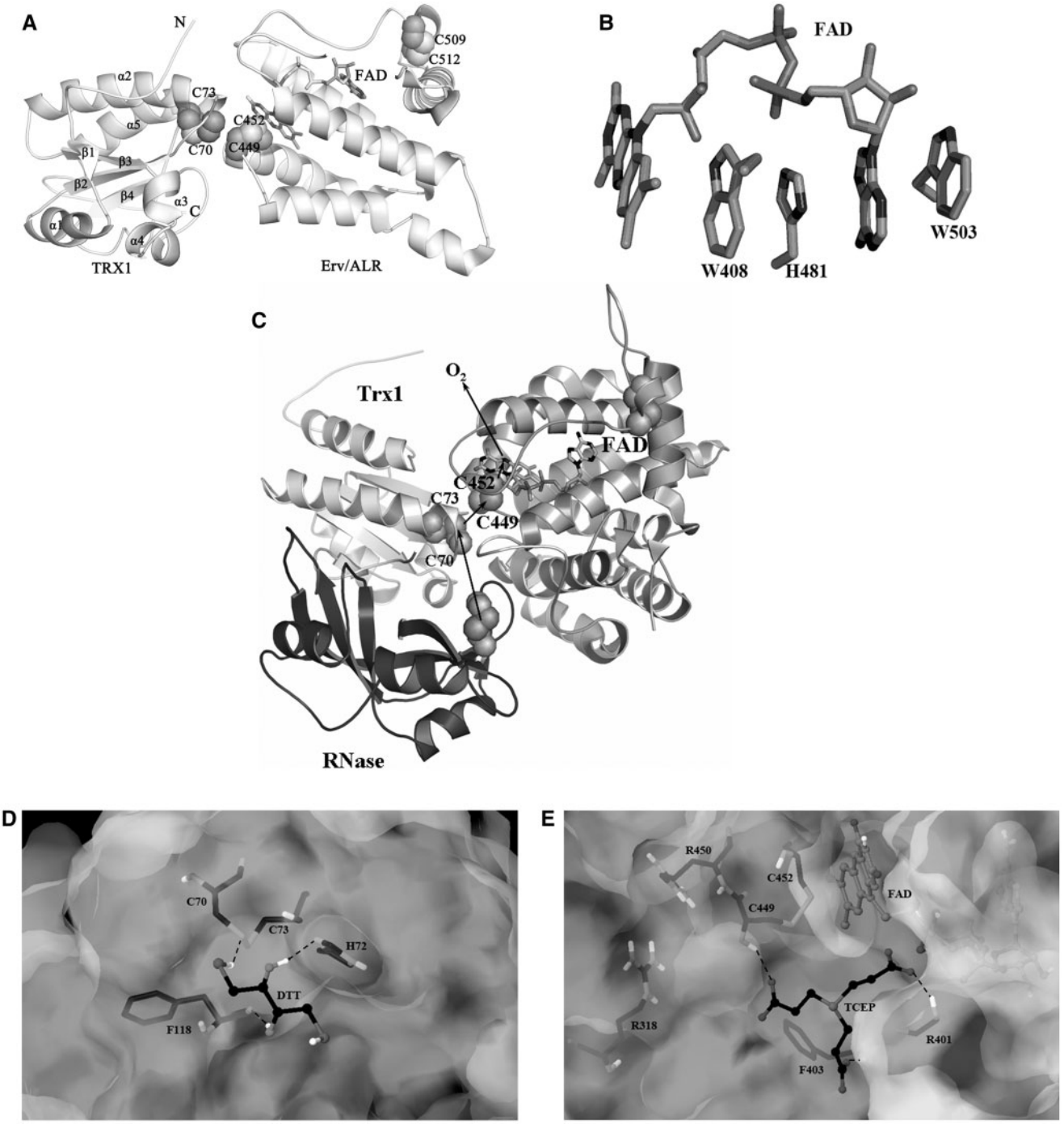

Fig. 3 The 3D structures of Trx1 and Erv/ALR domains and the interaction mode of HsQSOX1b with RNase, DTT and TCEP. (A) Docking result of modelled Trx1 module and crystal structure of human QSOX 1b (PDB code: 3LLI). The functional essential cysteines forming disulphide bonds were represented by spheres. The secondary structure elements of thioredoxin fold in Trx1 was labelled. (B) The aromatic ring stacking in Erv/ALR domain of QSOX. The isoalloxazine ring and adenine ring of FAD stack with rings of Trp408, His481 and Trp503. (C) RNase-QSOX docking model. The probable electron transfer pathways were represented by arrow directions. Docking results of DTT (D) and TCEP (E) were also shown. Hydrogen bond was labelled by dash lines. The binding site of the small-molecule substrate was shown in surface. The property changed from hydrophobicity to hydrophilicity by the surface colour from light to dark.

suggested there were more complicated mechanisms and electron transfer pathways when QSOX catalysed substrate to form disulphide bond formation or be oxidized. Our data suggests that there should be different electron transfer pathways during the oxidation of thiol-containing reductants or non-thiol reductant TCEP, as described in Fig. 4. The first pathway shows that the electron was transferred from the thiol-containing substrates to the C70–C73 motif, further to the C449–C452 motif, then to FAD and finally to oxygen when QSOX oxidizes reduced proteins and DTT. The second pathway shows that the electron can go from TCEP to the C449–C452 motif, further to FAD and finally to oxygen. This means that the

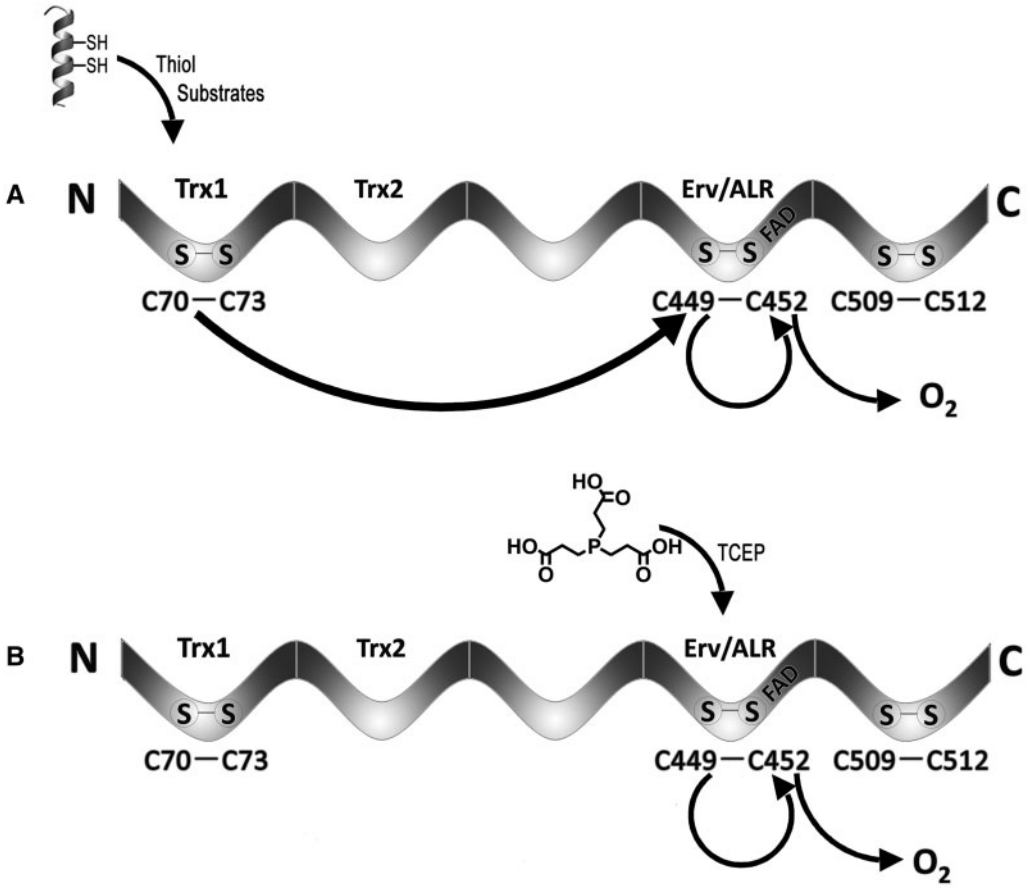

Fig. 4 Electron transfer pathway when QSOX oxidizing thiol-containing substrates DTT, rRNase and non-thiol substrate TCEP. (A) Showed the electron was transferred from thiol-containing substrates to C70–C73 motif, further to C449–C452 motif, then to FAD and finally to oxygen when QSOX oxidizing thiol-containing substrates. (B) Exhibited that the electron could go from TCEP to C449–C452 motif directly, further to FAD and finally to oxygen.

C70–C73 motif is only necessary for the oxidation of thiol-containing substrates rRNase and DTT but not for the non-thiol substrate TCEP.

Conclusion

Due to its unique protein structure, QSOX was the only thiol oxidase that could oxidize protein substrates efficiently and directly. However, the whole crystal structure of QSOX remains unknown. Here we constructed the 3D structural model of the Trx1 domain and did a series of molecular docking. Congruent results were obtained from both computer simulation and biological experiments. The results showed that the three CXXC motifs of HsQSOX1b played different roles in the oxidation of the disulphide reductants. C70–C73 disulphide was essential in transferring disulphide bond from thiol-containing substrates reduced proteins and DTT to C449–C452 of the Erv/ALR domain, but did not participate in the oxidation of TCEP. C449–C452 was the driver of the activity of HsQSOX1b and participated in the oxidation of reductant substrates. The vicinal disulphide C509–C512, distal from the active centre, was not involved in the electron transfer process during substrate oxidation. Based on the above results we propose that two electron transfer pathways exist during the oxidation of thiol-containing substrates and non-thiol substrates, separately.

Funding

863 Program (grant no. 2006AA02Z160); Program for New Century Excellent Talents in University (grant no. NCET-06-0415); Fok Ying Tung Education Foundation (grant no. 111022); NSFC (grant no. 30500102); NSFC (grant no. 90713026); The 111 Project (grant no. B07023).

Conflict of interest

None declared.

References

1. Ostrowski, M.C. and Kistler, W.S. (1980) Properties of a flavoprotein sulfhydryl oxidase from rat seminal vesicle secretion. *Biochemistry* **19**, 2639–2645
2. Brohawn, S.G., Miksa, I.R., and Thorpe, C. (2003) Avian sulfhydryl oxidase is not a metalloenzyme: adventitious binding of divalent metal ions to the enzyme. *Biochemistry* **42**, 11074–11082
3. Raje, S. and Thorpe, C. (2003) Inter-domain redox communication in flavoenzymes of the quiescin/sulfhydryl oxidase family: role of a thioredoxin domain in disulfide bond formation. *Biochemistry* **42**, 4560–4568

4. Hoober, K.L., Joneja, B., White, H.B. 3rd, and Thorpe, C. (1996) A sulfhydryl oxidase from chicken egg white. *J. Biol. Chem.* **271**, 30510–30516
5. Hoober, K.L., Sheasley, S.L., Gilbert, H.F., and Thorpe, C. (1999) Sulfhydryl oxidase from egg white. A facile catalyst for disulfide bond formation in proteins and peptides. *J. Biol. Chem.* **274**, 22147–22150
6. Hoober, K.L. and Thorpe, C. (1999) Egg white sulfhydryl oxidase: kinetic mechanism of the catalysis of disulfide bond formation. *Biochemistry* **38**, 3211–3217
7. Gross, E., Sevier, C.S., Vala, A., Kaiser, C.A., and Fass, D. (2002) A new FAD-binding fold and intersubunit disulfide shuttle in the thiol oxidase Erv2p. *Nat. Struct. Biol.* **9**, 61–67
8. Wu, C.K., Dailey, T.A., Dailey, H.A., Wang, B.C., and Rose, J.P. (2003) The crystal structure of augmenter of liver regeneration: a mammalian FAD-dependent sulfhydryl oxidase. *Protein Sci.* **12**, 1109–1118
9. Vitu, E., Bentzur, M., Lisowsky, T., Kaiser, C.A., and Fass, D. (2006) Gain of function in an ERV/ALR sulfhydryl oxidase by molecular engineering of the shuttle disulfide. *J. Mol. Biol.* **362**, 89–101
10. Heckler, E.J., Alon, A., Fass, D., and Thorpe, C. (2008) Human quiescin-sulfhydryl oxidase, QSOX1: probing internal redox steps by mutagenesis. *Biochemistry* **47**, 4955–4963
11. Raje, S., Glynn, N.M., and Thorpe, C. (2002) A continuous fluorescence assay for sulfhydryl oxidase. *Anal. Biochem.* **307**, 266–272
12. UniprotKB. http://www.uniprot.org/
13. Marsden, R.L., McGuffin, L.J., and Jones, D.T. (2002) Rapid protein domain assignment from amino acid sequence using predicted secondary structure. *Protein Sci.* **11**, 2814–2824
14. Sali, A. and Blundell, T.L. (1993) Comparative protein modelling by satisfaction of spatial restraints. *J. Mol. Biol.* **234**, 779–815
15. Tian, G., Xiang, S., Noiva, R., Lennarz, W.J., and Schindelin, H. (2006) The crystal structure of yeast protein disulfide isomerase suggests cooperativity between its active sites. *Cell* **124**, 61–73
16. Thompson, J.D., Gibson, T.J., Plewniak, F., Jeanmougin, F., and Higgins, D.G. (1997) The CLUSTAL_X windows interface: flexible strategies for multiple sequence alignment aided by quality analysis tools. *Nucleic Acids Res.* **25**, 4876–4882
17. Laskowski, R., Macarthur, M., Moss, D., and Thornton, J. (1993) PROCHECK: a program to check the stereochemical quality of protein structures. *J. Appl. Cryst.* **26**, 283–291
18. Alon, A., Heckler, E.J., Thorpe, C., and Fass, D. (2010) QSOX contains a pseudo-dimer of functional and degenerate sulfhydryl oxidase domains. *FEBS Lett.* **584**, 1521–1525
19. Dominguez, C., Boelens, R., and Bonvin, A.M. (2003) HADDOCK: a protein–protein docking approach based on biochemical or biophysical information. *J. Am. Chem. Soc.* **125**, 1731–1737
20. de Vries, S.J., van Dijk, A.D., Krzeminski, M., van Dijk, M., Thureau, A., Hsu, V., Wassenaar, T., and Bonvin, A.M. (2007) HADDOCK versus HADDOCK: new features and performance of HADDOCK2.0 on the CAPRI targets. *Proteins* **69**, 726–733
21. Schneidman-Duhovny, D., Inbar, Y., Nussinov, R., and Wolfson, H.J. (2005) PatchDock and SymmDock: servers for rigid and symmetric docking. *Nucleic Acids Res.* **33**, W363–W367
22. Duhovny, D., Nussinov, R., and Wolfson, H.J. (2002) Efficient Unbound Docking of Rigid Molecules. *Proceedings of the 2'nd Workshop on Algorithms in Bioinformatics (WABI)*, Rome, Italy, Lecture Notes in Computer Science 2452 (Gusfield *et al.*, eds.), pp. 185–200, Springer Verlag
23. MacroModel, version 9.6, Schrödinger, LLC, New York, NY, 2008
24. SiteMap, version 2.2, Schrödinger, LLC, New York, NY, 2008
25. Glide, version 5.0, Schrödinger, LLC, New York, NY, 2008
26. Lee, J., Hofhaus, G., and Lisowsky, T. (2000) Erv1p from Saccharomyces cerevisiae is a FAD-linked sulfhydryl oxidase. *FEBS Lett.* **477**, 62–66
27. Gerber, J., Muhlenhoff, U., Hofhaus, G., Lill, R., and Lisowsky, T. (2001) Yeast ERV2p is the first microsomal FAD-linked sulfhydryl oxidase of the Erv1p/Alrp protein family. *J. Biol. Chem.* **276**, 23486–23491
28. Stein, G. and Lisowsky, T. (1998) Functional comparison of the yeast scERV1 and scERV2 genes. *Yeast* **14**, 171–180
29. Hoober, K.L., Glynn, N.M., Burnside, J., Coppock, D.L., and Thorpe, C. (1999) Homology between egg white sulfhydryl oxidase and quiescin Q6 defines a new class of flavin-linked sulfhydryl oxidases. *J. Biol. Chem.* **274**, 31759–31762
30. Benayoun, B., Esnard-Feve, A., Castella, S., Courty, Y., and Esnard, F. (2001) Rat seminal vesicle FAD-dependent sulfhydryl oxidase. Biochemical characterization and molecular cloning of a member of the new sulfhydryl oxidase/quiescin Q6 gene family. *J. Biol. Chem.* **276**, 13830–13837
31. Coppock, D.L., Cina-Poppe, D., and Gilleran, S. (1998) The quiescin Q6 gene (QSCN6) is a fusion of two ancient gene families: thioredoxin and ERV1. *Genomics* **54**, 460–468
32. Herrmann, J.M., Kauff, F., and Neuhaus, H.E. (2009) Thiol oxidation in bacteria, mitochondria and chloroplasts: common principles but three unrelated machineries? *Biochim. Biophys. Acta* **1793**, 71–77
33. Thorpe, C., Hoober, K.L., Raje, S., Glynn, N.M., Burnside, J., Turi, G.K., and Coppock, D.L. (2002) Sulfhydryl oxidases: emerging catalysts of protein disulfide bond formation in eukaryotes. *Arch. Biochem. Biophys.* **405**, 1–12